FRACTURE ENERGY OF STEEL FIBRE REINFORCED CONCRETE

J.A.O. Barros[(1)], J. Sena Cruz[(2)]
Dep. of Civil Eng. – School of Eng. – University of Minho
Campus de Azurém, 4810 Guimarães CODEX
([1]) barros@eng.uminho.pt
([2]) jsena@eng.uminho.pt

Summary: Steel fibre reinforced concrete (SFRC) is a cementitious material reinforced with discrete fibres. The energy absorption capacity is the main material property benefited by fibre reinforcement. Closed-loop servo-controlled equipment should be used to evaluate this property. The tests should be carried out using displacement control in order to obtain the post-peak force-displacement relationship (tensile strain-softening branch).

To assess the fracture energy of SFRC three point bending tests were carried out using displacement control. Series of notched beams reinforced with 30, 60 and 90 kg/m^3 of hooked ends steel fibres were tested. Besides the energy dissipated in fracturing the concrete, the energy determined from the force-displacement relationship can also include the energy absorbed during non-linear behaviour of concrete in compression. Ductile materials, like concrete reinforced with a high content of fibres, develop large deflections before exhausting their energy absorption capacity. In these cases, the "fixed" points of the bar supporting the displacement transducer may not remain fixed, adding an extra deflection into the control displacement transducer, thus, leading to incorrect evaluation of the fracture energy. These factors were analysed in the present work in order to assess the suitability of the specimen dimensions and the test procedures for evaluating the fracture energy of SFRC.

1 – INTRODUCTION

In the last two decades efforts have been made in order to achieve a total or a partial substitute of the conventional reinforcement for concrete. In this way, several discrete fibres were developed for concrete reinforcement, namely, steel, glass, synthetic and natural fibres [1,2]. Steel fibres are the most used in concrete applications due to the following main reasons: economy, manufacture facilities, reinforcing effects and resistance to the environment aggressiveness. Industrial floors, tunnelling lines and prefabrication are the main applications of steel fibre reinforced concrete (SFRC), where the conventional reinforcement is replaced by a given content of fibres [3,4].

The concrete property most benefited by fibre reinforcement is the energy absorption capacity [1,5,6]. Adding the amount of fibres used in current applications of SFRC, the concrete compression, tensile, shear and torsional strength are only marginally increased [1,2]. In structures with redundant supports, like slabs on soil and tunnelling lines, the increment on the material energy absorption capacity, provided by fibre reinforcement, enhances the cracking behaviour and increases the load bearing capacity of these structures [7,8]. Due to the relevance of the energy absorption capacity of fibrous concrete, several entities have been proposed for evaluating this property [5,9], namely, the toughness indices, the equivalent flexural strength and the fracture energy. Among these entities, the fracture energy is the most used in the constitutive models for characterizing the concrete tensile post-cracking behaviour [10-14]. The other entities have not been used widely in numerical simulation of the behaviour of *SFRC* structures [15].

The accuracy of a numerical simulation of the non-linear behaviour of concrete structures depends significantly on the material fracture energy, G_f, which is defined as the amount of energy necessary to create one unit area of a crack [16]. The fracture energy can be evaluated from uniaxial tensile tests or bending tests using displacement control. The uniaxial tensile test is the most appropriate, but the test stability requires a very stiff closed-loop servo-controlled testing system [17,18]. Besides the high costs of this equipment, the uniaxial tensile test requires very high precision measuring devices, which have to be fixed on appropriate locations of the specimen, and should be controlled by a sophisticated control unit. Such tests are very time consuming and require skilled technical staff [19]. Due to these drawbacks, three- or four-point bending tests on notched beams are usually carried out to evaluate the material fracture energy. The three-point bending tests on centre-notched beams are less used but are, perhaps, more suitable to characterise the fracture parameters of SFRC [20].

The present work describes the three-point bending tests carried out on notched beams of SFRC. Based on the data obtained, the bending stress in the notched cross section, the energy dissipated and the fracture energy were evaluated. The specimen dimensions and the test procedures proposed by RILEM [16] for evaluating the fracture energy of plain concrete may not be appropriate for fibrous concrete. Due to the higher deformability of SFRC compared with plain concrete, the energy dissipated by concrete in non-linear compression behaviour, and the displacements of the "fixed" points of the bar supporting the control displacement transducer may not be negligible. The significance of these effects on the evaluation of the fracture energy of *SFRC* is discussed in the present work.

2 – MATERIALS AND SPECIMENS

2.1 - Fibres

Steel fibres of 30 mm length, l_f, 0.5 mm diameter, d_f, with a fibre aspect ratio of $l_f/d_f = 30/0.5 = 60$, with the trademark Dramix ZP305, were used [21]. To avoid fibre alignment due to wall effect, the fibre type was chosen taking into account that its length should be less than 2.5 times the smaller dimension of the cross section of the bending specimens used for evaluating the energy absorption capacity of SFRC [1]. The fibres are glued together, side by side, into bundles of about 30 fibres with a water solvable glue in order to improve the mix workability and eliminating balling [1]. The main characteristics of the fibres are presented in Table 1.

Table 1 – Main characteristics of *Dramix* ZP30/.50 hooked ends steel fibres.

Type of fibre	Density (g/cm^3)	Tensile strength (MPa)	Elasticity modulus (GPa)	Ultimate strain (%)
ZP30/.50	7.8	1250	200	3 - 4

2.2 - Concrete

The concrete mix is indicated in Table 2. More details about the mix composition and the mixing procedures can be found elsewhere [22].

Table 2 – Concrete composition.

Element	Content (kg/m^3 of concrete)
Cement	450
Sand (0-5 mm)	729
Coarse aggregates (5-15)	1000
Water	202.5
Fibres	0, 30, 60, 90

The uniaxial compression strength, f_{cm}, the tangent modulus of elasticity, E_{ci}, and the reduced modulus of elasticity, E_{c1}, are presented in Table 3 [23]. These results are the average values of, at least, five cylinder specimens of 150 mm diameter and 300 mm height. The manufacturing of the specimens, the equipment and the test procedures for uniaxial compression tests were described elsewhere [22].

Table 3 – Compression strength and elasticity modulus.

Property	Content of fibres (kg/m^3)			
	0	30	60	90
Age (Days)	48	40	40	40
f_{cm} (MPa)	36.1	33.9	34.4	33.5
E_{ci} (GPa)	31.9	25.1	26.0	27.2
E_{c1} (GPa)	20.9	16.6	15.4	15.0

2.3 – Bending notched beam specimens

The specimens were compacted on a vibrating table in order to assure a dense mix and a uniform distribution of fibres. The specimens for bending tests have the dimensions

recommended by RILEM for evaluating the fracture energy of plain concrete [16], namely 800×100×100 mm^3. Since the ratio between the compressive and the tensile strength of the SFRC tested in this work is in the range of 5 to 10, the aforementioned specimen dimensions and the test procedures recommended by RILEM were used to evaluate the fracture energy [24]. The suitability of the specimen dimensions and the test procedures for evaluating the fracture energy of SFRC will be discussed hereafter.

The curing procedure consisted of the following: The first week in the curing chamber; water cured for 28 days and left in a curing chamber until one week before testing. In the last week the specimens were prepared for testing. At midspan, in the surface opposite to the casting surface, a saw cut of 5 mm wide by 25 mm in height was made with appropriate equipment (see Figure 1). The tests were carried out on specimens at the age of 400 to 500 days.

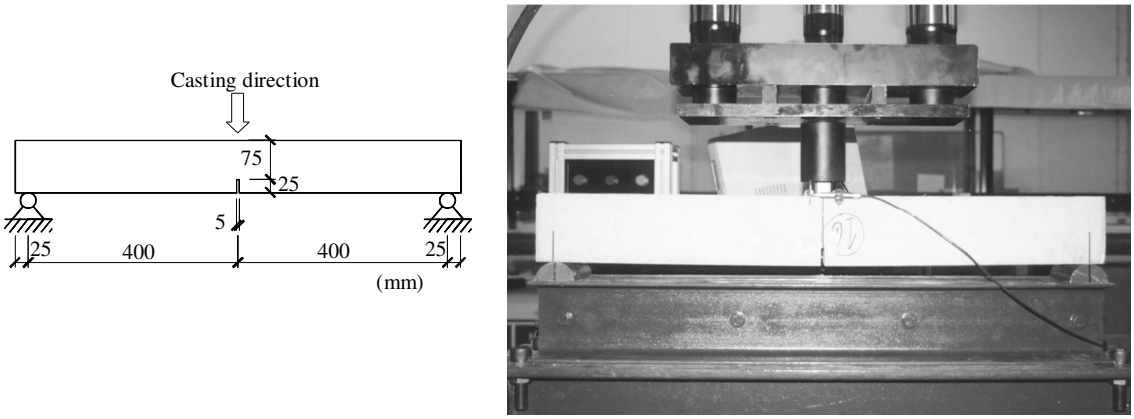

Figure 1 – Notched beam for three point bending tests.

3 – EQUIPMENT AND TEST PROCEDURES

A closed-loop servo-controlled testing system was developed for static and dynamic tests on specimens and structural elements [25]. The control unit of this equipment and the displacement, force and strain measurement devices are controlled by the software developed, which includes a friendly interface module for defining the test procedures.

The load was applied by a triple actuator of 250 kN maximum load capacity. The triple actuator is composed by three cylinders (see Figure 2), two with 100 kN maximum load capacity, placed at actuator extremities, named as lateral cylinders here, and one with 50 kN maximum load capacity, placed at the actuator centre, referred to as central cylinder. This actuator can work for loading limits of 250 kN, 200 kN and 50 kN, activating the three cylinders, the lateral cylinders or the central cylinder. In this way, the loading level can be selected, taking into account the predicted maximum load in the test, which enhances the test stability and the test control performance. This triple actuator can carry out stable tests on specimens of low bearing capacity, which is the case of the notched beam specimens. When the load is applied by the central cylinder (active cylinder), the lateral cylinders can introduce a pre-load into the central cylinder (see Figure 3a). Therefore, the null force in the active cylinders can be avoided, which contributes for test stability. The pre-load level can be selected on the software developed. In the same way, when the load is applied by the lateral cylinders (active cylinders), the central cylinder can introduce a pre-load into the lateral cylinders (see Figure 3b).

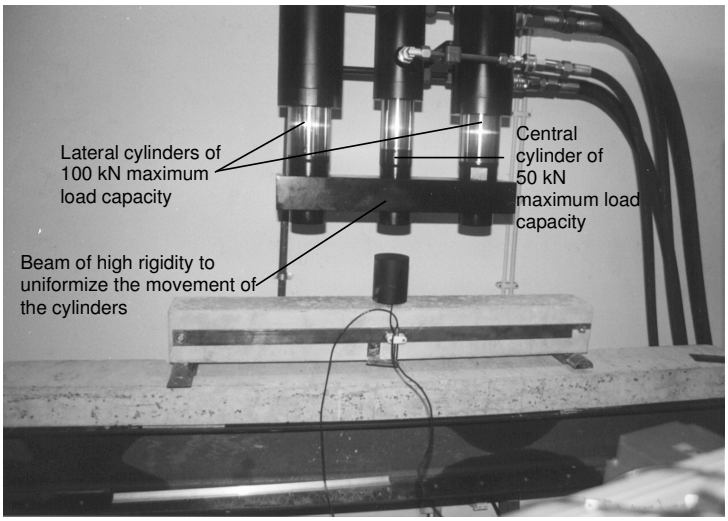

Figure 2 – Triple actuator.

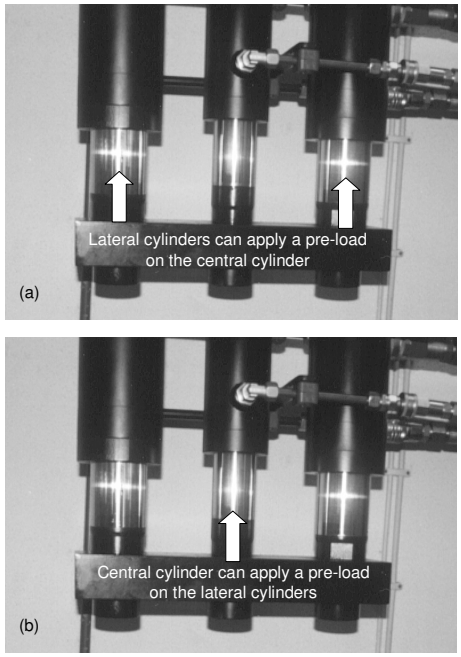

Figure 3 – Pre-loads that can be applied to the active cylinders.

To obtain the complete load-deflection relationship, the tests were carried out using displacement control. In order to avoid extraneous deformations, the middle point deflection was measured by a displacement transducer placed on a frame attached to the beam, the so-called "Japanese Yok" [5,9], see Figure 4. The displacement transducer has a linear branch of 25 mm with 0.06% accuracy of the full scale.

A tension-compression force transducer of 20 kN maximum load capacity and 0.5% accuracy was used to measure the force. The load was applied through fixtures which allowed for rotational freedom. A steel bar with dimensions of 95×20×20 mm^3 was placed between the actuator and the specimen to distribute the load on the beam's width (line load).

Figure 5 shows the structure supporting the test set-up. It consists of HEB 200 steel elements, setting up a frame that offers reaction to the actuator. The final configuration of the reaction frame was established after some preliminary tests that revealed the need for using very stiff reaction frames in order to assure the stability of this type of tests.

During the preliminary tests it was observed that the loop gain of the data acquisition board had to be increased when the ratio of the specimen stiffness and that of the supporting structure was increased.

The tests were carried out using the following deflection rates: 0.15 mm/minute up to 0.1 mm of deflection, 0.3 mm/minute between 0.1 and 0.2 mm and 0.6 mm/minute between 0.2 and 2.3 mm. Among the three loading regimes available on the triple actuator, the lowest was selected. In order to enhance the test stability, a pre-load of 16 kN was applied by the lateral cylinders to the active central cylinder. The force and the displacement were registered every second. The data was saved on a file for post-processing.

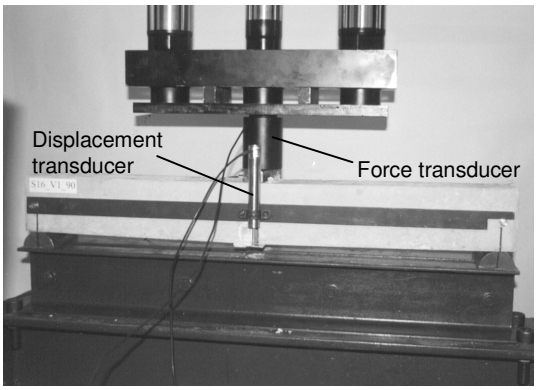

Figure 4 – Force and displacement measuring devices.

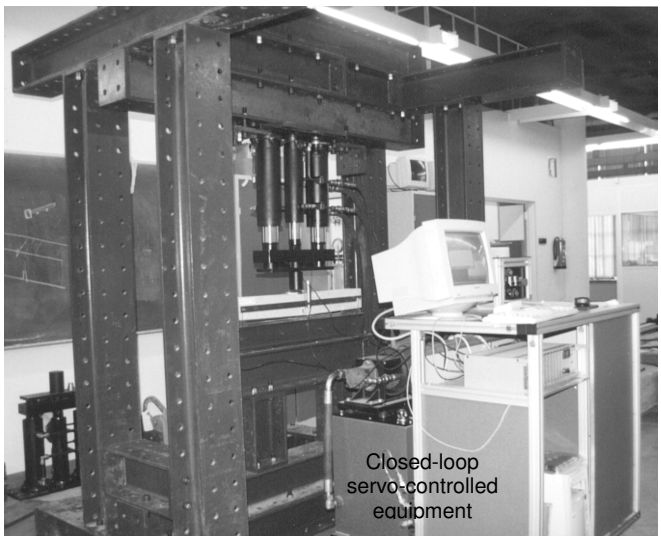

Figure 5 – Equipment and reaction frame.

4 – RESULTS

The force-deflection relationships obtained from the specimens reinforced with 30, 60 and 90 kg/m^3 of fibres are shown in Figures 6 to 8. The "average" force-deflection relationship for each series is depicted in Figure 9. For a given series, this relationship is obtained estimating, for each deflection, the average force of the tests in this series.

The maximum force and the maximum stress at notched cross section, for the three fibre contents are represented in Figures 10 and 11. The maximum stress at notched cross section is evaluated using the following expression

$$f_{net} = \frac{3}{2}\frac{F_{\max} L}{b(h-a)^2} \tag{1}$$

where F_{max} is the maximum load, L=800 mm is the specimen span, b=100 mm and h=100 mm are the width and the height of the specimen and a=25 mm is the depth of the notch.

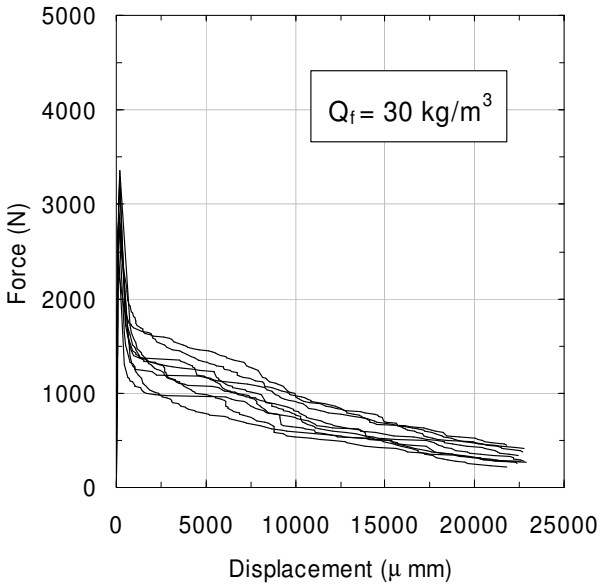

Figure 6 – Force-deflection relationship for series of 30 kg/m^3 of fibres.

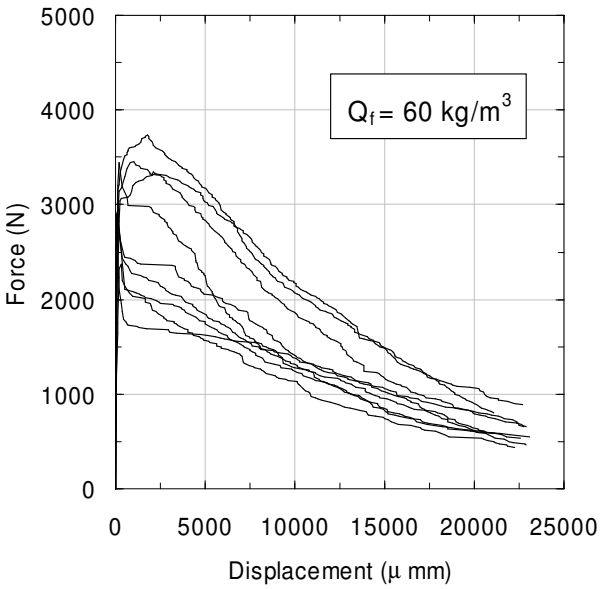

Figure 7 – Force-deflection relationship for series of 60 kg/m^3 of fibres.

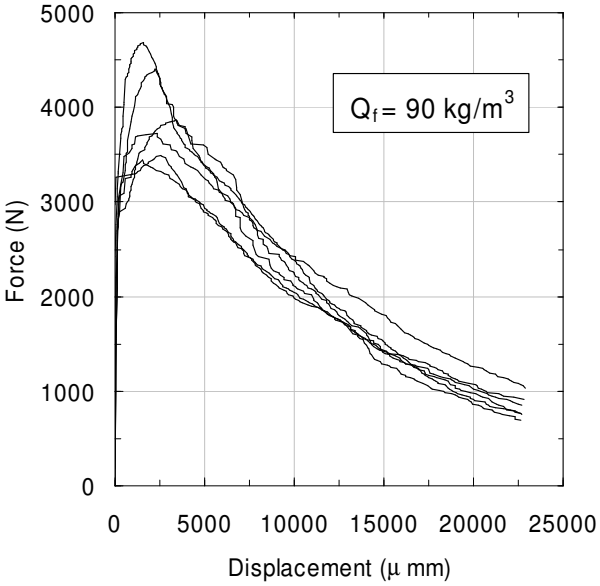

Figure 8 – Force-deflection relationship for series of 90 kg/m^3 of fibres.

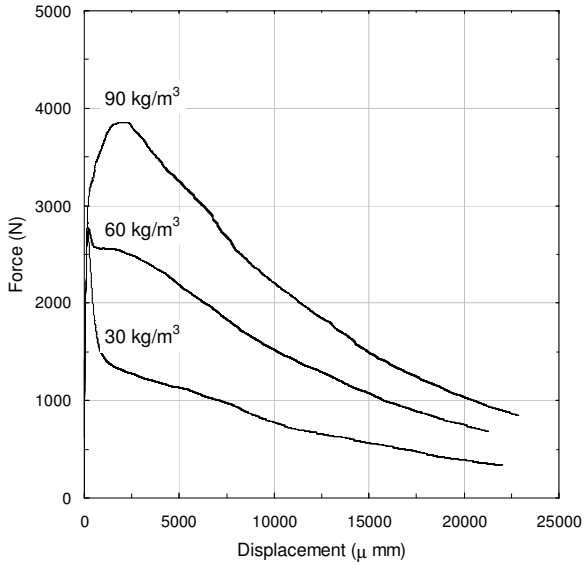

Figure 9 – "Average" force-displacement relationship for series of 30, 60 e 90 kg/m^3 of fibres.

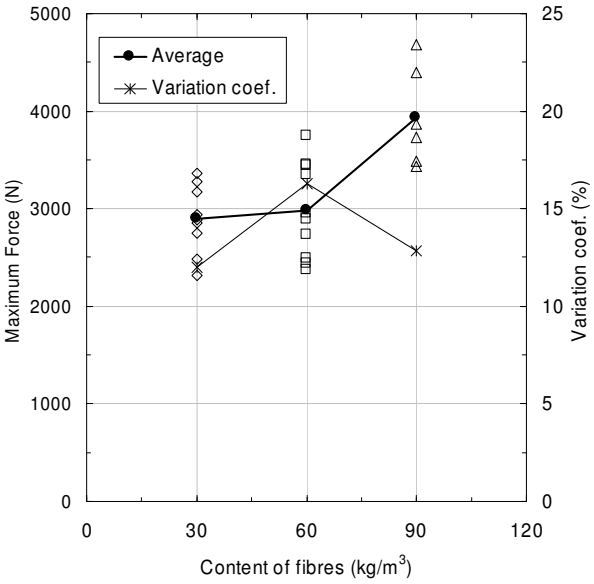

Figure 10 – Maximum force.

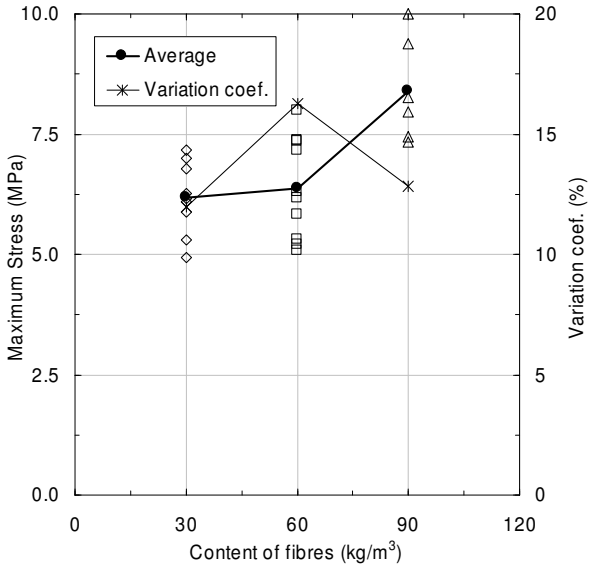

Figure 11 – Maximum stress at notched cross section.

The main results obtained are presented in Table 4. A maximum stress, at notched cross section, of 4.6 MPa and an energy of 1690 Nmm were obtained in plain concrete specimens of a mix design indicated in Table 2. These specimens were $450\times150\times150$ mm^3 with a notch depth of 75 mm.

Table 4 – Maximum force and stress values obtained.

Content of fibres (kg/m^3)	Maximum force (N)	Maximum stress at notched cross section (MPa)
30	2894	6.2
60	2983	6.4
90	3935	8.5

From the results obtained, the following can be pointed out:

- A significant dispersion of the results is observed, mainly in specimens reinforced with 60 kg/m^3 of fibres, which reveals the need for improving the procedures of mixing in order to assure a homogeneous distribution of fibres;
- The maximum load in series reinforced with 30 and 60 kg/m^3 of fibres is almost the same;
- The maximum load increases significantly in specimens reinforced with 90 kg/m^3 of fibres;
- The decline of the force after peak load decreases with the increment of fibre content;
- In specimens reinforced with 90 kg/m^3 of fibres a hardening branch is developed after the first crack deflection, due to the high percentage of fibres bridging the crack surfaces.

Influence of the movement of the "fixed" points of the bar supporting the displacement transducer

In bending tests with specimens that can develop large deflections before exhausting their energy absorption capacity, the two "fixed" points of the bar supporting the control displacement transducer (see Figure 4) do not remain fixed, as it is schematically illustrated in Figure 12. If specimens are supported in rollers, which is the usual practice, these two points go upward with the deflection of the specimen, adding a supplementary displacement to the control displacement transducer. This supplementary displacement can be measured from two displacement transducers placed at these "fixed" points and should be deducted from the displacement registered in the control transducer. Otherwise, the

energy absorption capacity evaluated from the force-deflection relationship will be larger than the real one.

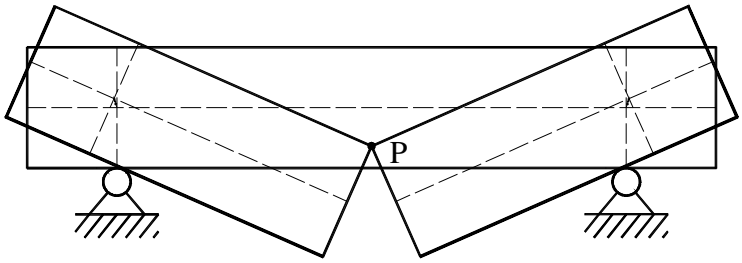

Figure 12 – The "fixed" points of the bar supporting the control displacement transducer do not remain fixed for large deflections.

In the present work the displacement of the "fixed" points of the bar is evaluated assuming the specimen as a two rigid blocks rotating in turn of the point P (see Figure 12). This displacement is deducted from the deflection registered in the control displacement transducer. For specimen dimensions used in the present work the displacement of the "fixed" points is 0.164 mm for a deflection of 20 mm, which is only 0.8% of this deflection. However, for specimens with dimensions of 450×150×150 mm^3, currently adopted for evaluating the toughness indices [5,9], a displacement of 0.9 mm of the "fixed" points was measured for a deflection of 20 mm (4.5%), which should not be neglected [6].

Table 5 includes the energy due to the displacement of the "fixed" points of the "Japanese Yok" bar. It can be concluded that, for the specimen dimensions and notch depth adopted, this energy is small. Since the approach used for evaluating the displacements of the "fixed" points gives an upper bound value, this energy will be even smaller.

Table 5 – The influence of the energy evaluated from the movement of the "fixed" points of the bar.

Content of fibres (kg/m^3)	U_L (1) (N.mm)	U_R (2) (N.mm)	$\frac{\lvert U_L - U_R \rvert}{U_R} \times 100$ (%)
30	18300	18180	0.84
60	34050	33770	0.82
90	49350	49000	0.72

(1) U_L - Energy evaluated from the registered force-deflection relationship

(2) U_R - Energy evaluated from the force-corrected deflection relationship

Figure 13 depicts the energy dissipated for the series tested. This energy is evaluated from the force-corrected deflection relationship up to a corrected deflection of about 23 mm. It is observed that, for fibre contents between 30 and 90 kg/m^3 the increment on the energy is almost linear. This tendency has already been observed in a previous work [13]. The dispersion of the results is also remarkable, mainly in series reinforced with 60 kg/m^3 of fibres.

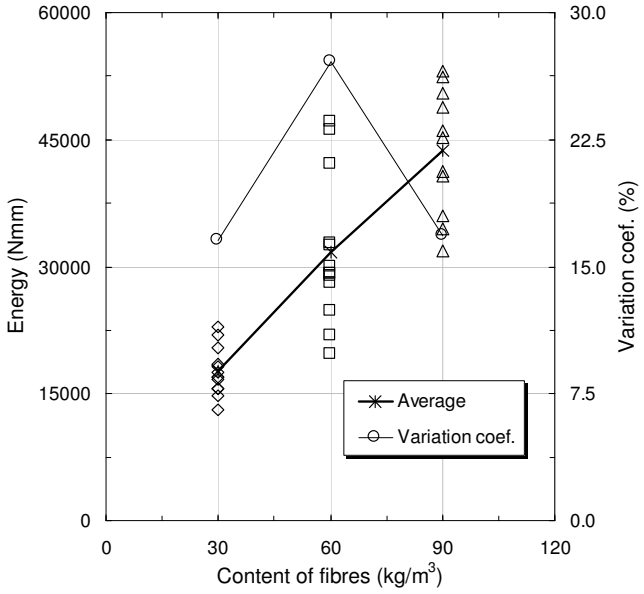

Figure 13 – Energy dissipated.

Influence of the concrete in non-linear compression behaviour

For large deflections the compression strain in the concrete volume, near the loaded area, may be greater than the linear elastic compression strain limit of SFRC. For ductile fibrous concrete specimens, the energy dissipated in non-linear compression behaviour can be significant, mainly, when the notch depth is less than half the height of the specimen [26]. This energy should be evaluated and deducted from the energy estimated using the force-deflection relationship. The energy dissipated by concrete in non-linear compression behaviour can be evaluated by the use of experimental or numerical tools. Adopting an experimental approach, displacement transducers should be placed in the upper one third of the specimen height, and the volume of concrete in non-linear compression behaviour should be also measured. In the numerical approach the energy dissipated by concrete in compression can be evaluated using a model that accounts for the material constitutive laws. This procedure was adopted in the present work and is described in the next section.

5 – EVALUATING THE FRACTURE ENERGY

To evaluate the fracture energy from the force-deflection relationship obtained in bending tests, the energy dissipated by concrete in non-linear compression behaviour should be determined. In order to estimate this energy the cross sectional layer model, schematically represented in Figure 14, was applied. According to this model, a cross section is discretized into concrete layers and a moment-curvature relationship is obtained, imposing cinematic and equilibrium equations, and considering the compression and tension constitutive laws developed for SFRC [13]. A full description of the model can be found elsewhere [14].

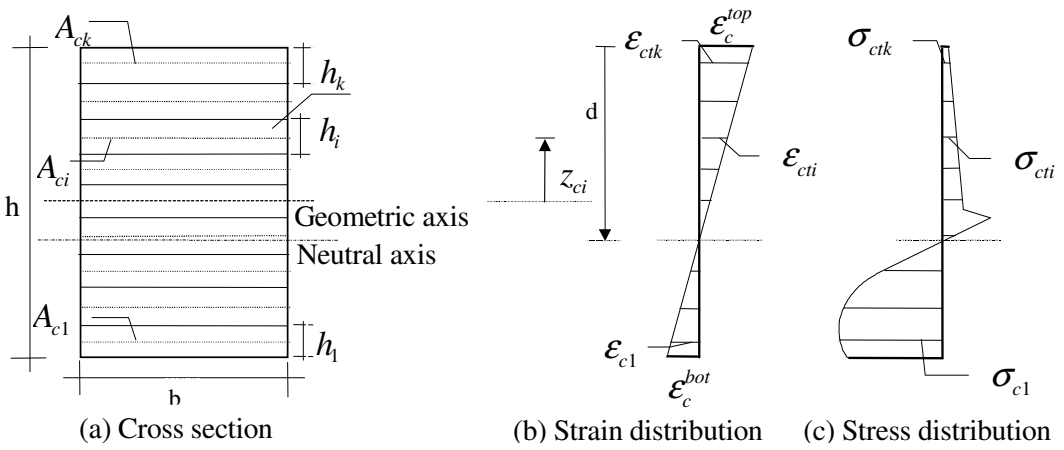

Figure 14 – Cross section discretization and assumed strain and stress diagrams.

In the approach adopted, the beam is assumed as two linear elastic blocks (zones of intact concrete) connected by a damaged zone, ahead of the notch (see Figure 15). The damaged zone is the volume of concrete where the energy is dissipated by the concrete cracking process and by the non-linear behaviour of concrete in compression. The width of the damaged zone is determined using the cross sectional layer model, fitting the experimental force-deflection data (see Figure 17). To calculate the width of the damaged zone it was assumed that it has constant width, L_{dz}. However, for evaluating the energy dissipated by concrete in non-linear compression behaviour a more realistic shape of the damage zone, represented in Figure 16, was adopted. According to this assumption the width of the damaged zone increases linearly from the mouth of the notch to the upper surface, and has the value of L_{dz} at the middle height of the net section.

Using the cross sectional layer model and discretizing the damaged zone in ten layers of equal thickness, a damaged zone width of 70 mm for the three series of tests was obtained.

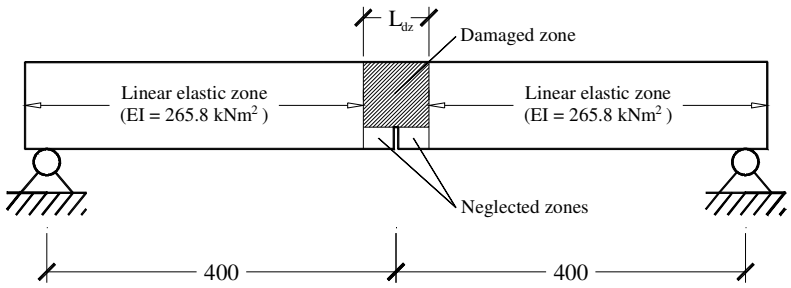

Figure 15 – Specimen idealisation for model use.

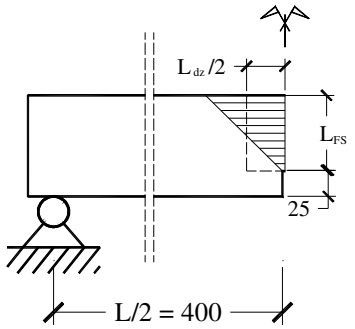

Figure 16 – Damaged zone discretized in ten concrete layers.

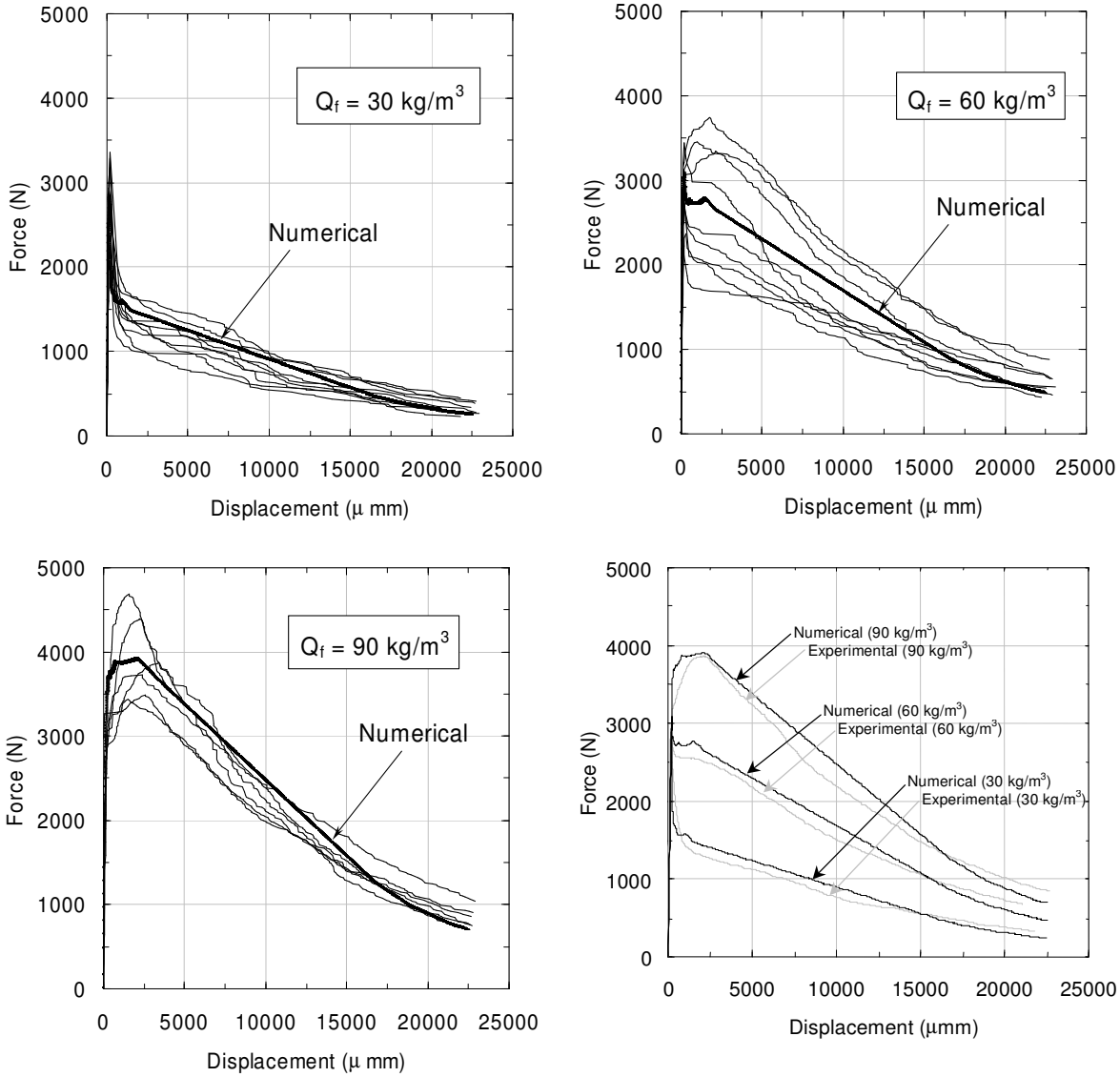

Figure 17 – Comparison between the results obtained with the cross sectional layer model and the experimental data.

Figure 18 represents schematically the procedure used to evaluate the energy dissipated by concrete in non-linear compression behaviour, and Table 6 includes the values obtained.

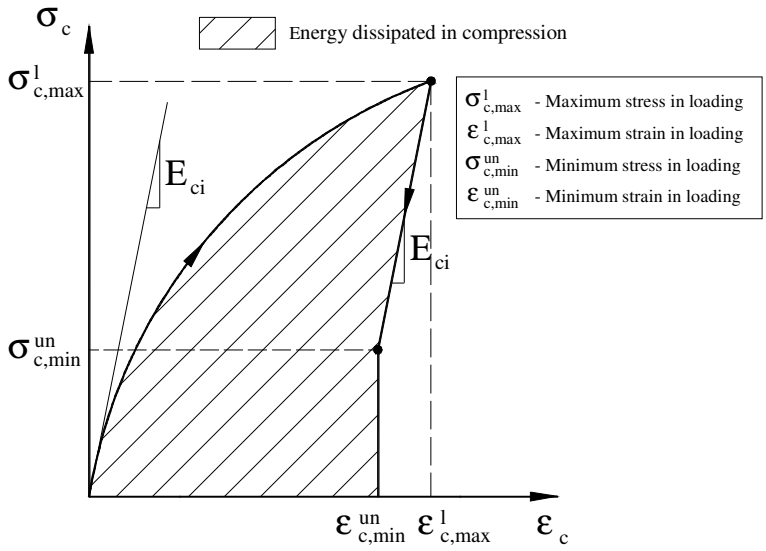

Figure 18 – Procedure to evaluate the energy dissipated by concrete in non-linear compression behaviour.

It is shown that, even for the series reinforced with the higher content of fibres, the energy dissipated by concrete in compression is less than 1% of the total energy, revealing that the specimen dimensions are adequate for evaluating the fracture energy of the fibrous composites studied.

Table 6 – Energy dissipated by concrete in non-linear compression behaviour.

Content of fibres (kg/m^3)	U_c (1) (N.mm)	$\frac{U_c}{U_R}\times 100$ (2) (%)	$G_f = \frac{U_R - U_c}{L_{FS}}$ (3) (N/mm)
30	40	0.22	2.419
60	160	0.47	4.481
90	450	0.92	6.473

(1): Energy dissipated in compression

(2): U_R is the total energy (see table 5)

(3): Fracture energy (L_{FS} is the fracture surface)

The fracture energy also presented in Table 6 is determined using the following expression

$$G_f = \frac{U_R - U_c}{L_{FS}} = \frac{U_{cr}}{L_{FS}} \tag{2}$$

where U_{cr} is the energy dissipated in fracturing the concrete and L_{FS} is the fracture surface of 75×100 mm^2. Figure 19 represents the fracture energy for the series tested.

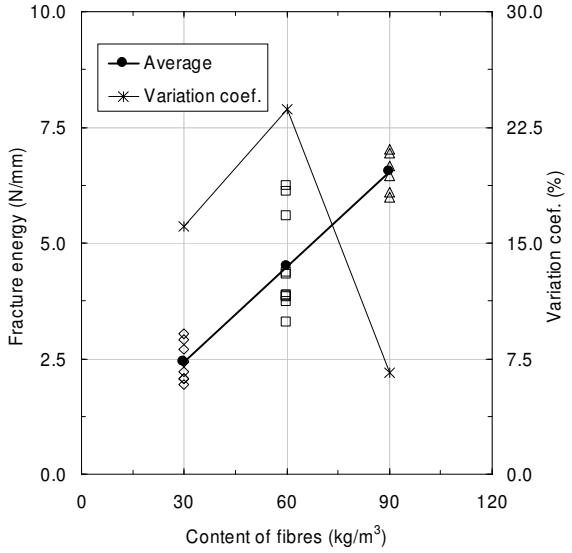

Figure 19 – Fracture energy.

Between 30 and 90 kg/m^3 of fibres, the fracture energy increases linearly with the fibre content, which is in agreement with previous results [13].

7 – CONCLUSIONS

Three point bending tests were performed for assessing the fracture energy of steel fibre reinforced concrete (SFRC). Series of notched beams of concrete reinforced with 30, 60 and 90 kg/m^3 of hooked-ends steel fibres were carried out using a closed-loop servo-controlled testing system. The main aspects influencing the evaluation of the fracture energy were discussed, namely, the mobility of the "fixed" points of the bar supporting the control displacement transducer and the energy dissipated by the concrete in non-linear compression behaviour.

From the results obtained, a significant increase in the maximum stress at the notched cross section was only observed on specimens reinforced with 90 kg/m^3 of fibres. The energy absorption capacity increased almost linearly with the fibre content, in agreement with results already published. The difficulties in assuring a homogeneous fibre distribution in concrete were highlighted by the dispersion of the results obtained.

Using specimens of 800×100×100 mm^3 and a notch of 25 mm in depth it was noted that the maximum displacement of the "fixed" points of the bar supporting the displacement transducer was less than 1.0% of the ultimate deflection. Due to the displacement of these "fixed" points, an extra deflection is added to the deflection measured by the control displacement transducer, which introduces parasite energy. However, for the specimen proposed, this energy is less than 1.0% of the energy estimated from the force-deflection relationship.

A cross sectional layer model was applied for evaluating the energy dissipated by concrete in non-linear compression behaviour. It was noted that, for the specimen used, this energy was less than 1% of the total energy determined from the force-deflection relationship. It can be concluded that the specimen dimensions and the test procedures adopted in the present work are suitable for evaluating the fracture energy in concrete of normal strength, reinforced with the type of fibre used, and in contents less than 100 kg/m^3.

8 – BIBLIOGRAFIA

[1] – ACI 544.1R-96, 'State-of-the-Art Report on Fiber Reinforced Concrete', *ACI Manual of Concrete Practice – Part 5 – ACI International*, 66 pp., 1997.

[2] – P.N. Balaguru and S.P. Shah, *Fiber reinforced cement composites*, McGraw-Hill International Editions, Civil Engineering Series, 1992.

[3] – A. Nanni and A. Johari, "RCC pavement reinforced with steel fibers", *Concrete International*, 64-69, April, 1989.

[4] – P.C. Tatnall and L. Kuitenbrouwer, "Steel fiber reinforced concrete in industrial floors", *Concrete International*, 43-47, December, 1992.

[5] – V.S. Gopalaratnam *et al.*, "Fracture toughness of fiber reinforced concrete", *ACI Materials Journal*, 88(4), 339-353, July-August, 1991.

[6] – J.A.O. Barros, *Comportamento do betão reforçado com fibras - análise experimental e simulação numérica* PhD thesis, Faculty of Eng., University of Porto, 1995. (in Portuguese)

[7] – J.A.O. Barros and J.A. Figueiras, "Experimental behaviour of fibre concrete slabs on soil", *Journal Mechanics of Cohesive-frictional Materials,* Vol. 3, 277-290, 1998.

[8] – J.A.O. Barros, "Experimental behavior of mesh reinforced shotcrete and steel fiber reinforced shotcrete panels", *International Conference of the European Ready Mixed Concrete Organization, ERMCO'98*, Lisboa, 23-27 Junho, 1998.

[9] – JSCE - The Japan Society of Civil Engineers, *Part III - 2 method of tests for steel fiber reinforced concrete*, Concrete Library of JSCE, Nº 3, 1984.

[10] – A. Hillerborg, "Analysis of fracture by means of the fictitious crack model, particularly for fibre reinforced concrete", *The International Journal of Cement Composites*, 2(4), 177-184, 1980.

[11] – R. De Borst, *Non-linear analysis of frictional materials*, PhD thesis, Delft Univ. of Technology, 1986.

[12] – J.G. Rots, *Computational modeling of concrete fracture*, PhD thesis, Delft University of Technology, 1988.

[13] – J.A.O. Barros and J. A. Figueiras, "Flexural behavior of steel fiber reinforced concrete: testing and modelling", *Journal of Materials in Civil Engineering, ASCE*, 11(4), ??, 1999.

[14] – J.A.O. Barros and J. A. Figueiras, "Nonlinear analysis of steel fibre reinforced concrete slabs on grade", *Computers & Structures*. (accepted for publication in 2000).

[15] – Dramix *Steel fibre reinforced industrial floor design in accordance with the Concrete Society TR34*, N.V. Bekaert S.A., Responsible editor: H. Thooft - Zingem 1997.

[16] – RILEM TC 50-FMC, "Determination of fracture energy of mortar and concrete by means of three-point bend tests on notched beams", *Materials and Structures*, 18(106), 285-290, 1985.

[17] – D.A. Hordijk, *Local approach to fatigue of concrete*, PhD Thesis, Delft University of Technology 1991.

[18] – Y. Wang, V.C. Li and S. Backer, "Experimental determination of tensile behaviour of fibre reinforced concrete", *ACI Materials Journal*, 87(5), 461-468, September-October, 1990.

[19] – J.A.O. Barros *et al.* "Tensile behaviour of glass fibre reinforced concrete", Recent Advances in Experimental Mechanics, eds. J.F. Silva Gomes *et al.*, Vol. 2, 1073-1080, 1994.

[20] – V.S. Gopalaratnam and R. Gettu, "On the characterization of flexural toughness in FRC", Workshop on Fibre Reinforced Cement and Concrete, Sheffield, U.K., July 28-30, 1984.

[21] – Bekaert Specification, *Dramix fibres hors fils d'acier pour reinforcement de betón et mortier*, Bekaert N.V., 1991.

[22] – J.M. Sena Cruz, *Comportamento cíclico de estruturas porticadas de betão armado reforçadas com fibras de aço*, Master Science Thesis, Faculty of Eng., University of Porto, 1998. (In Portuguese)

[23] - CEB-FIP Model Code 1990 *Comite Euro-International du Beton*, Bulletin d'Information nº 213/214, Ed. Thomas Telford, 1993.

[24] – A. Hillerborg, *Concrete fracture energy tests performed by 9 laboratories according to a draft RILEM recommendation*, Report to RILEM TC50-FMC, Report TVBM-3015, Lund Sweden, 1983.

[25] – F. Freitas, J.A.O. Barros and P. Fonseca, *Manual de utilizador do equipamento SENTUR - release 1.0*, Dep. of Civil Eng., School of Eng., University of Minho, 1998. (In Portuguese)

[26] – A. Hillerborg, *Influence of beam size on concrete fracture energy determined according to a draft RILEM recommendation*, Report to RILEM TC50-FMC, report TVBM-3021, Lund Sweden, 1985.